Acquisition of in vivo MR spectroscopy

All in vivo MR scans were performed on 3 T Tim Trio scanners (Siemens, Erlangen), using a head 32-channel phased array for receive and body radio-frequency (RF) coil for transmit. Single voxel spectroscopy was performed using recently optimized 1D LASER (*34*) and the 2D LASER-COSY (*16*) sequences. In addition, a newly designed 1D MEGA-LASER was used for spectral-editing (fig. S1). Typical voxel sizes were 27 cm^3 ($3\times3\times3$ cm^3) or 42.8 cm^3 ($3.5\times3.5\times3.5$ cm^3), in case of large tumors. A repetition time (TR) of 1.5s was used for all acquisitions. For 1D LASER and 2D LASER-COSY an echo time (TE) of 45 ms was used. The 1D MEGA-LASER spectra were acquired with TE of 75 ms.

Processing, analysis, and quantification of in vivo MR spectroscopy

Raw data were exported from the Siemens scanners for subsequent processing and analysis. The 1D LASER data (FID) were processed and quantified with LCModel (*12*) using a GAMMA-simulated basis set for LASER. For 1D MEGA-LASER data fitting was done in jMRUI (*13*). For 2D LASER-COSY, the FIDs of all t1 increments were imported in Matlab (The Mathworks) and futher processed. For quantification and comparison of methods and subjects, the 2HG/(Glu+Gln) ratio was chosen.

List of Supplementary Material:

Methods and Materials

Fig. S1. Pulse sequence diagram for the 1D MEGA-LASER spectral editing experiment.

Fig. S2. Phantom experiments and simulations for 2D LASER-COSY and 1D LASER at 3T.

Fig. S3. Optimization of the 1D MEGA-LASER spectral editing on phantoms at 3T.

Fig. S4. 1D HRMAS spectra recorded at 14T and 3 kHz MAS on a biopsy sample from one patient with R132H IDH1 anaplastic astrocytoma.

Fig. S5. LCModel fitting of the 1D LASER spectrum from the R132C IDH1 anaplastic astrocytoma patient.

Fig. S6. LCModel fitting of the 1D LASER spectrum from a wild-type IDH1 primary gliobalstoma patient.

Fig. S7. LCModel fitting of the 1D LASER spectrum from a wild-type IDH1 healthy volunteer.

Fig. S8. LCModel fitting of the 1D LASER spectrum from the tumor voxel of the R132H IDH1 secondary glioblastoma patient.

Fig. S9. LCModel fitting of the 1D LASER spectrum from the healthy side voxel of the R132H IDH1 secondary glioblastoma patient.

REFERENCES AND NOTES

1. D. W. Parsons, S. Jones, X. S. Zhang, J. C. H. Lin, R. J. Leary, P. Angenendt, P. Mankoo, H. Carter, I. M. Siu, G. L. Gallia, A. Olivi, R. McLendon, B. A. Rasheed, S. Keir, T. Nikolskaya, Y. Nikolsky, D. A. Busam, H. Tekleab, L. A. Diaz, J. Hartigan, D. R. Smith, R. L. Strausberg, S. K. N. Marie, S. M. O. Shinjo, H. Yan, G. J. Riggins, D. D. Bigner, R. Karchin, N. Papadopoulos, G. Parmigiani, B. Vogelstein, V. E. Velculescu, K. W. Kinzler, *Science* **321**, 1807 (Sep, 2008).
2. L. Chin, M. Meyerson, K. Aldape, D. Bigner, T. Mikkelsen, S. VandenBerg, A. Kahn, R. Penny, M. L. Ferguson, D. S. Gerhard, G. Getz, C. Brennan, B. S. Taylor, W. Winckler, P. Park, M. Ladanyi, K. A. Hoadley, R. G. W. Verhaak, D. N. Hayes, P. T. Spellman, D. Absher, B. A. Weir, L. Ding, D. Wheeler, M. S. Lawrence, K. Cibulskis, E. Mardis, J. H. Zhang, R. K. Wilson, L. Donehower, D. A. Wheeler, E. Purdom, J. Wallis, P. W. Laird, J. G. Herman, K. E. Schuebel, D. J. Weisenberger, S. B. Baylin, N. Schultz, J. Yao, R. Wiedemeyer, J. Weinstein, C. Sander, R. A. Gibbs, J. Gray, R. Kucherlapati, E. S. Lander, R. M. Myers, C. M. Perou, R. McLendon, A. Friedman, E. G. Van Meir, D. J. Brat, G. M. Mastrogianakis, J. J. Olson, N. Lehman, W. K. A. Yung, O. Bogler, M. Berger, M. Prados, D. Muzny, M. Morgan, S. Scherer, A. Sabo, L. Nazareth, L. Lewis, O. Hall, Y. M. Zhu, Y. R. Ren, O. Alvi, J. Q. Yao, A. Hawes, S. Jhangiani, G. Fowler, A. San Lucas, C. Kovar, A. Cree, H. Dinh, J. Santibanez, V. Joshi, M. L. Gonzalez-Garay, C. A. Miller, A. Milosavljevic, C. Sougnez, T. Fennell, S. Mahan, J. Wilkinson, L. Ziaugra, R. Onofrio, T. Bloom, R. Nicol, K. Ardlie, J. Baldwin, S. Gabriel, R. S. Fulton, M. D. McLellan, D. E. Larson, X. Q. Shi, R. Abbott, L. Fulton, K. Chen, D. C. Koboldt, M. C. Wendl, R. Meyer, Y. Z. Tang, L. Lin, J. R. Osborne, B. H. Dunford-Shore, T. L. Miner, K. Delehaunty, C. Markovic, G. Swift, W. Courtney, C. Pohl, S. Abbott, A. Hawkins, S. Leong, C. Haipek, H. Schmidt, M. Wiechert, T. Vickery, S. Scott, D. J. Dooling, A. Chinwalla, G. M. Weinstock, M. O'Kelly, J. Robinson, G. Alexe, R. Beroukhim, S. Carter, D. Chiang, J. Gould, S. Gupta, J. Korn, C. Mermel, J. Mesirov, S. Monti, H. Nguyen, M. Parkin, M. Reich, N. Stransky, L. Garraway, T. Golub, A. Protopopov, I. Perna, S. Aronson, N. Sathiamoorthy, G. Ren, H. Kim, S. K. Kong, Y. H. Xiao, I. S. Kohane, J. Seidman, L. Cope, F. Pan, D. Van Den Berg, L. Van Neste, J. M. Yi, J. Z. Li, A. Southwick, S. Brady, A. Aggarwal, T. Chung, G. Sherlock, J. D. Brooks, L. R. Jakkula, A. V. Lapuk, H. Marr, S. Dorton, Y. G. Choi, J. Han, A. Ray, V. Wang, S. Durinck, M. Robinson, N. J. Wang, K.

MATERIALS and METHODS

Selection of human subjects

Patients and healthy volunteers listed in Table 2 were scanned with informed consent approved by the Internal Review Board at our institution. Patients were diagnosed by an experienced neuropathologist who examined formalin-fixed paraffin-embedded samples from the subjects that had been stained with hematoxylin and eosin (H&E). In total, 10 subjects (2 mutant $IDH1_{R132}$ glioma patients, 4 wt-*IDH1* glioma patients, and 4 wt-*IDH1* healthy volunteers) were scanned with in vivo MRS.

Biopsy collection for HRMAS and LC-MS

Biopsies (n= 10, Table 1) were collected at the time of surgery and snap frozen in liquid nitrogen. Informed consent was obtained before surgery for biopsy collection. Biopsies were obtained from 7 glioma patients: 5 primary glioblastoma (wt-*IDH1*) and 2 anaplastic astrocytoma (1 patient with $IDH1_{R132H}$, and 1 patient with wt-*IDH1*). In addition, non-tumor healthy control biopsies were obtained from 3 patients that had been surgically treated for epilepsy.

Genetic analysis for *IDH1* mutation

A multiplexed allele-specific assay (*1*) was used to detect somatic mutations in tumor DNA extracted from formalin-fixed paraffin-embedded samples. The assay, SNaPshot Version 2 (Life Technologies/Applied Biosystems), detects mutations in 60 different loci from 14 cancer genes. Briefly, multiplex PCR using tumor DNA is followed by mutation analysis using single-base extension sequencing technology that generates allele-specific, fluorescently labeled probes. The average sensitivity of detecting mutations in this assay has been established at approximately 5% mutant allele (*1*).

Brain phantoms

Two phantoms with a mixture of metabolites were prepared for the initial assessment of unambiguous 2HG detection with MRS. One phantom contained normal brain

metabolites at physiological concentrations 12.5 mM of NAA, 10 mM of creatine hydrate (Cre), 3 mM of choline chloride (Cho), 7.5 mM of myo-inositol (Myo), 7.5 mM of L-glutamic acid (Glu), 1 mM of GABA, 5 mM of D,L-lactic acid (Lac). Another phantom contained the same brain metabolites as the first phantom, but also had 3 mM of D-2HG (D-α-hydroxyglutaric acid disodium salt, Sigma Aldrich). A series of phantoms containing only 2HG at different concentrations (1, 2, 4, 8, and 16 mM) were prepared for calibration and sensitivity tests. Each phantom was measured three times, randomly in a test and retest experiment that included taking out the phantoms from the scanner. All phantoms were doped with sodium azide (0.1%) to prevent bacterial growth; pH-buffered by adding 50 mM of potassium phosphate monobasic, 56 mM of sodium hydroxide; and spiked with 1 ml/l of Gd-DPTA (gadolinium diethylenetriamine penta-acetic acid, Magnevist) to obtain in vivo–like T_1 relaxation times.

The first phantom (brain metabolites without 2HG) was a large sphere of 16 cm diameter that is used routinely for calibration of our MR scanners. All the phantoms containing 2HG consisted in smaller spheres of 5 cm diameter that were placed and secured tightly inside larger cylindrical containers of 10 cm diameter filled with saline solution. Smaller spheres were used in order to minimize the quantity of 2HG required; placing them inside larger containers filled with saline helped with shimming and adjustments of transmit power. The 1D LASER (*2*), 1D MEGA-LASER, and 2D LASER-COSY (*3*) acquisition and processing was performed as mentioned for the in vivo MRS.

Simulations of metabolite spectra

Quantum mechanical simulations were done in GAMMA [General Approach To Magnetic Resonance Mathematical Analysis (*4*)] for spectra of 2HG and the overlapping brain metabolites Glu, Gln, and GABA. The simulations were done using piece-wise constant Hamiltonian (20 ms time step) for the 1D LASER (*2*) sequence, assuming 3 T main magnetic field and literature NMR parameters (*5, 6*) for the metabolites. The same pulse and gradient waveforms as used on the MR scanners were programmed in GAMMA.

Ex vivo HR-MAS NMR spectroscopy

All HR-MAS experiments were conducted on a wide-bore 14.1 T (600 MHz ^{1}H) Bruker Avance spectrometer using a 4 mm double channel HR-MAS probehead (Bruker) equipped with a deuterium lock channel. Small samples weighting 2-4 mg were cut from the frozen biopsies and introduced in 4-mm ZrO_2 rotors before complete thawing, and were secured with a top insert, screw and cap (Bruker). The probehead was pre-cooled to -8° C and the temperature was accurately maintained by a variable temperature unit (VTU) during measurements in order to minimize sample degradation. All measurements were made at 3 kHz MAS. 2D TOBSY (20) was performed with an adiabatic $C9^{1}_{15}$ sequence (45ms mixing time) that improves crosspeaks and signal-to-noise ratio on biopsies. Rotor synchronized (278ms) adiabatic WURST-8 pulses (32) were used for building WiW symmetry block elements. Acquisition parameters of 2D TOBSY spectra included: 2,000 points along the direct t2 dimension (13 ppm spectral window), 200 points along the indirect t1 dimension (7.5 ppm spectral window) with time proportional phase increments (TPPI) for phase-sensitive spectra, 8 averages, 4 dummy scans (for the first t1), repetition time of 2s, total acquisition time of 53.3 min. Processing was performed with the Bruker's spectrometer XWINNMR 3.5 software, and included phase sensitive real Fourier transformation (FT), linear prediction forward to 1k points in the t1 dimension, sine-square window in both dimensions, baseline correction in both dimensions. 2D TOBSY spectra were assigned, quantified and plotted using SPARKY program (T. D. Goddard and D. G. Kneller, SPARKY 3, UCSF). The minimum contour level was set to be five times the noise floor as determined by SPARKY. 1D spectra were obtained with direct excitation (pulse and acquire) and CPMG [Carr-Purcell-Meiboom-Gill (*7*)] of 50 rotor-synchronized echoes (fig. S4). Rectangular 90° and 180° hard pulses had 8 μs and 16 μs, respectively. FIDs were acquired with 8k points (13 ppm spectral window), and 1 Hz exponential multiplication was used for processing. In addition to HRMAS on biopsies, spectra from the second phantom (brain metabolites and 2HG) were collected at 14.1 T. A 5 mm double channel liquid-state probehead equipped with a deuterium lock channel was used. A volume of 0.8 ml from the second phantom was placed in a 5 mm NMR glass tube. 2D Total Correlation Spectroscopy (TOCSY) (*8*) with an adiabatic MLEV-16 sequence (*9, 10*) and 1D direct excitation spectra were acquired.

Similar acquisition and processing parameters as mentioned in the case of biopsies were used. In all experiments on biopsies and phantom, presaturation for 1 s with low power continuous wave was used to suppress water, and the B_0 field was locked by the deuterium signal (0.2 ml D_2O was added to all samples).

LC-MS of brain biopsies

The same biopsies measured by HRMAS were used for LC-MS metabolic profiling (*11*). Metabolite extraction was accomplished by adding a 10× volume (m/v ratio) of -80 °C methanol:water mix (80:20) to the brain tissue (approximately 20-40 mg) followed by 30 s homogenization at 4 °C. These chilled, methanol-extracted homogenized tissues were then centrifuged at 14,000 rpm for 30 min to sediment the cellular and tissue debris and the cleared tissue supernatants were transferred to a screw-cap freezer vial and stored at -80 °C. For analysis, a 2× volume of tributylamine (10 mM) acetic acid (10 mM) pH 5.5 was added to the samples and analysed by LC–MS as follows. Sample extracts were filtered using a Millex-FG 0.20 μm disk and 10 μl were injected onto a reverse-phase HPLC column (Synergi 150 mm × 2 mm, Phenomenex) and eluted using a linear gradient LC–MS-grade methanol (50%) with 10 mM tributylamine and 10 mM acetic acid, ramping to 80% methanol:10 mM tributylamine: 10 mM acetic acid over 6 min at 200 μl/min. Eluted metabolite ions were detected using a triple-quadrupole mass spectrometer, tuned to detect in negative mode with multiple-reaction-monitoring mode transition set according to the molecular masses and fragmentation patterns for eight known central metabolites, including 2-HG. Data were processed using Analyst Software (Applied Biosystems) and metabolite signal intensities were obtained by standard peak integration methods.

Acquisition of in vivo MR spectroscopy

All in vivo MR scans were performed on 3 T Tim Trio scanners (Siemens, Erlangen), using a head 32-channel phased array for receive and body radio-frequency (RF) coil for transmit. Single voxel spectroscopy was performed using recently optimized 1D LASER (*2*) and the 2D LASER-COSY (*3*) sequences. In addition, a newly designed 1D MEGA-LASER was used for spectral-editing (fig. S1). The same LASER module was used for

localization in all sequences because of sharp excitation margins, minimal chemical shift displacement error, reduced lineshape modulation, insensitivity to B_1 inhomogeneity and flip angles errors. Low power, gradient offset independent adiabaticity wurst modulated (GOIA-W(16,4), Ref. (*2*)) pulses were employed with 3.5 ms duration, 20 kHz bandwidth, and 0.817 kHz maximum B_1 field amplitude. Typical voxel sizes were 27 cm^3 (3×3×3 cm^3) or 42.8 cm^3 (3.5×3.5×3.5 cm^3), in case of large tumors. A repetition time (TR) of 1.5s was used for all acquisitions. For 1D LASER and 2D LASER-COSY an echo time (TE) of 45 ms was used. 1D LASER spectra were collected with 128 averages (acquisition time of 3.2 min), the 2D LASER-COSY spectra were acquired with 64 t1 increments (10 ppm f1 spectral window), 8 averages per t1 increment, and 4 dummy scans for the first t1 (acquisition time of 12.8 min). The f2 directly acquired spectral dimension was set to 1.25 kHz (~10ppm) and the free induction decay (FID) had 512 points in all experiments. The 1D MEGA-LASER spectra were acquired with TE of 75 ms, and 200 averages were collected (acquisition time of 5 min). In all sequences, water suppression was performed using WET (*12*) scheme. Automatic shimming of the single voxels was performed using FASTESTMAP (*13*) to ensure linewidths of 6-12 Hz in human subjects. Anatomical MR images were collected to guide the position of MRS voxels. For patients the preferred modality was axial fluid-attenuated inversion recovery (FLAIR) acquired with TR 10 s, TE 70 ms, and 5 mm slice thickness (1 mm gap), and 0.6×0.45 mm^2 in-plane resolution, 23 slices, 384×512 matrix (imaging time 3.03 min). For healthy volunteers a multi-echo MEMPRAGE (*14*) volumetric acquisition was performed, with 1 mm isotropic voxels, TR = 2.53 s, TE1/TE2/TE2/TE3/TE4 = 1.64/3.5/5.36/7.22 ms, inversion time TI = 1.2 s (imaging time 6.1 min). Voxels on healthy volunteers were placed in similar regions as observed on patients to match coil sensitivity profile and regional metabolic differences.

Processing, analysis, and quantification of in vivo MR spectroscopy

Raw data were exported from the Siemens scanners for subsequent processing and analysis. The 1D LASER data (FID) were processed and quantified with LCModel (*15*) using a GAMMA-simulated basis set for LASER. FT, phase correction and baseline correction was performed as part of the LCModel processing. For 1D MEGA-LASER

data the FT, phase correction, baseline correction, and line fitting were done in jMRUI (*16*). For 2D LASER-COSY, the FIDs of all 64 t1 increments were imported in Matlab (The Mathworks). Processing steps included: 1) FT along t2; 2) linear prediction forward to 128 points in t1 using the ITMPM method (*17*); 3) FT along t1; and 4) square-sine window function in both f_1 and f_2 dimensions in order to improve crosspeaks, and reduce diagonal ringing and baseline distortion. The 2D spectra were displayed as contour levels in magnitude mode, with the first contour level chosen five times the floor noise level as estimated from standard deviation of noise floor in a signal free spectral region (0.5–0 ppm/0.5—0 ppm, f_1/f_2). A minimum SNR of 5 was considered for reliable identification of crosspeaks from the noise. This was decided based on the series of 2HG phantoms. At 1 mM, the H_α crosspeaks had an SNR of ~2.5, which was considered insufficient to distinguish them from noise. Metabolites were assigned based on the literature (*5, 6, 18*) values for their NMR parameters, and crosspeak volumes were integrated in Matlab.

For quantification, the 2HG/(Glu+Gln) ratio was chosen for the following reasons: 1) 2HG, Glu and Gln have a similar five-spin system, hence the buildup of their COSY crosspeaks and spectral-edited peaks is similar; 2) Glu and Gln are largely present both in tumors and healthy brain, yielding clearly resolved crosspeaks and spectral-edited peaks; 3) the absolute quantification based on internal water can not be used in tumors where water content varies largely; and 4) 2HG quantification relative to Glu and Gln is preferred over quantification relative to creatine (*19*), because creatine does not have crosspeaks and may vary with disease.

Supplementary Figures

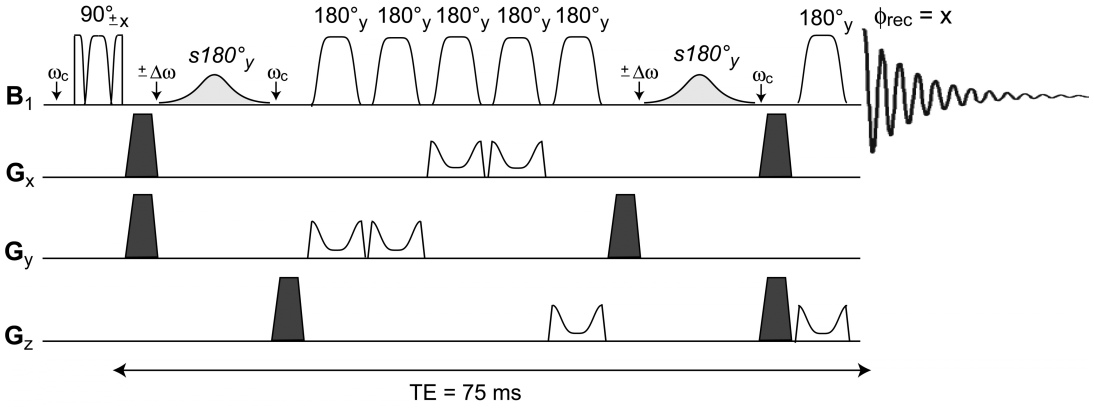

Fig. S1. Pulse sequence diagram for the 1D MEGA-LASER spectral editing experiment. Two 180° frequency selective pulses (*s180°*) are inserted in the LASER sequence after the first 90° excitation pulse and before the last 180° slice selective pulse, respectively. The *s180°* are Gaussian pulses with a bandwidth of 60 Hz, which are applied symmetrically from the water peak (4.7 ppm) at ±Δω offsets (±2.8 ppm, or 1.9 ppm and 7.5 ppm on an absolute scale). All the other pulses are applied at a carrier frequency (ω_c) of 2.9 ppm in the middle of the 2HG spectrum. The phase of the first 90° pulse is alternated ±x simultaneously with the ±Δω offset of the Gaussian pulses, while the receiver and the other pulse have the same phases. The spoiler gradients needed for spectral-editing are shown in dark black and have a trapezoidal shape, amplitude of 20 mT/m, duration of 2.5 ms, ramps of 750 μs. The GOIA-W(16,4) pulses used for slice selection are the same used for the LASER sequence from (*2*), with a duration of 3.5 ms, 20 kHz bandwidth, 0.81 kHz amplitude, and gradient ramps of 600 μs. An echo time of 75 ms is possible with these parameters which was found to be optimal optimum for 2HG (see fig. S3). Notations: TE = echo time; ϕ_{rec} = receiver phase; B_1 = radiofrequency field; $G_{x,y,z}$ = gradients on the three orthogonal axis.

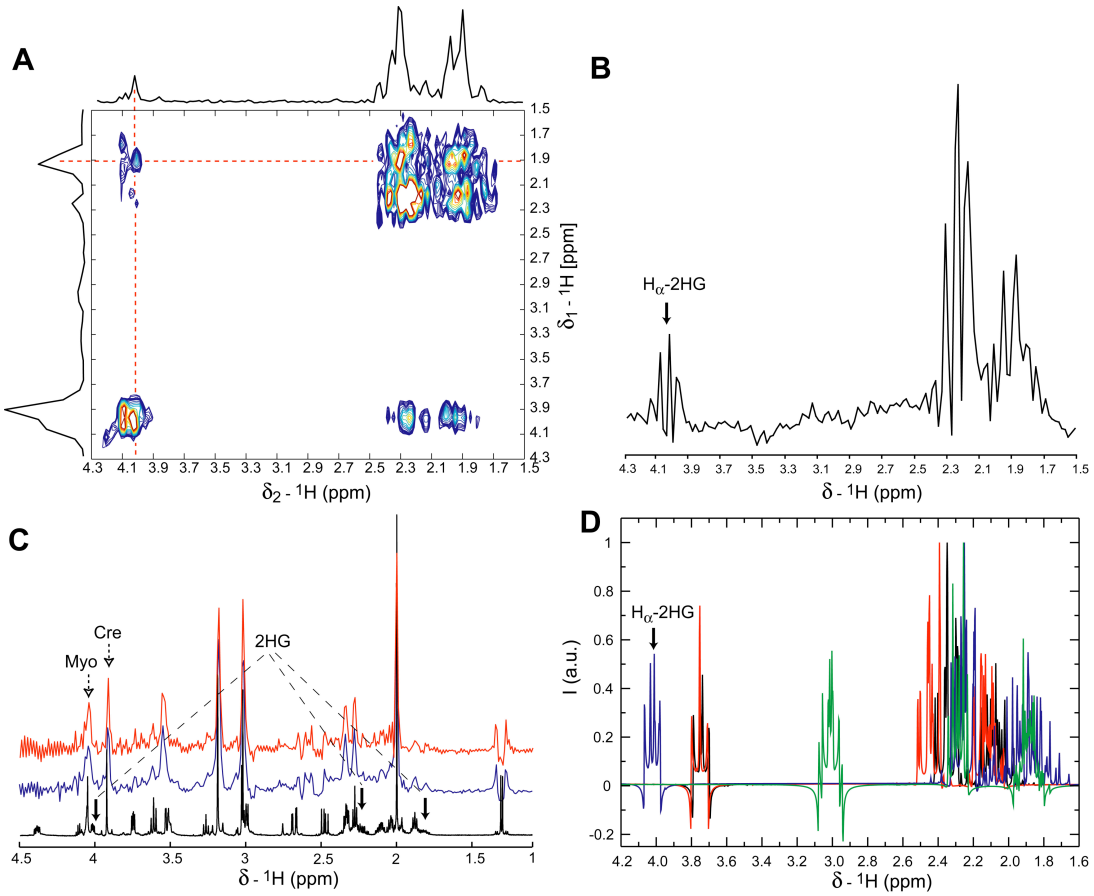

Fig. S2. Phantom experiments and simulations for 2D LASER-COSY and 1D LASER at 3T. (**A** and **B**) 2D LASER-COSY spectra (A) and 1D LASER spectrum (B) from a phantom containing 16 mM of 2HG, recorded at 3T on clinical MR scanners. Projections through the Hα-Hβ crosspeak of 2HG (4.02/1.91 (δ_2/δ_1) ppm) are shown next to the 2D spectrum. (**C**) 1D LASER spectra recorded at 3T from the phantom containing normal brain metabolites (red trace) and the phantom containing the mixture of 2HG and normal brain metabolites (blue trace). A spectrum of the phantom containing 2HG and brain metabolites recorded at 14T is shown in black. Arrows indicate the position of 2HG lines, Myo and Cre. (**D**) Quantum mechanical simulations of 1D LASER spectra at 3T show the overlap of 2HG (blue), Glu (black), Gln (red), and GABA (green). Simulations also show minimal line shape modulation of the multiplets due to good refocusing of the scalar coupling evolution by LASER sequence, which helps fitting and quantification.

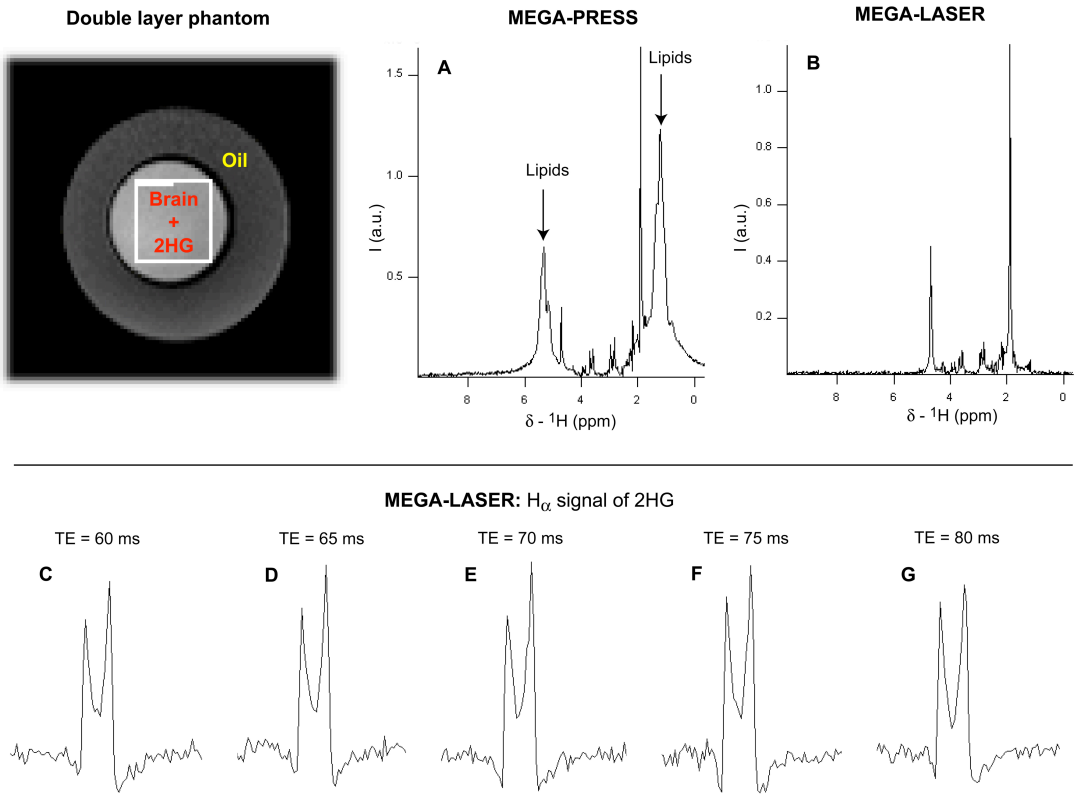

Fig. S3. Optimization of the 1D MEGA-LASER spectral editing on phantoms at 3T. Localization and echo time of MEGA-LASER sequence were optimized in a double layer phantom that contained an inner sphere of brain metabolites at physiological concentration with 2HG (3 mM) added, and an outer layer of oil. Arrows indicate contamination with lipid signal from outside the voxel in MEGA-PRESS (**A**). The same voxel of 3×3×3 cm^3 was used in MEGA-PRESS and MEGA-LASER.

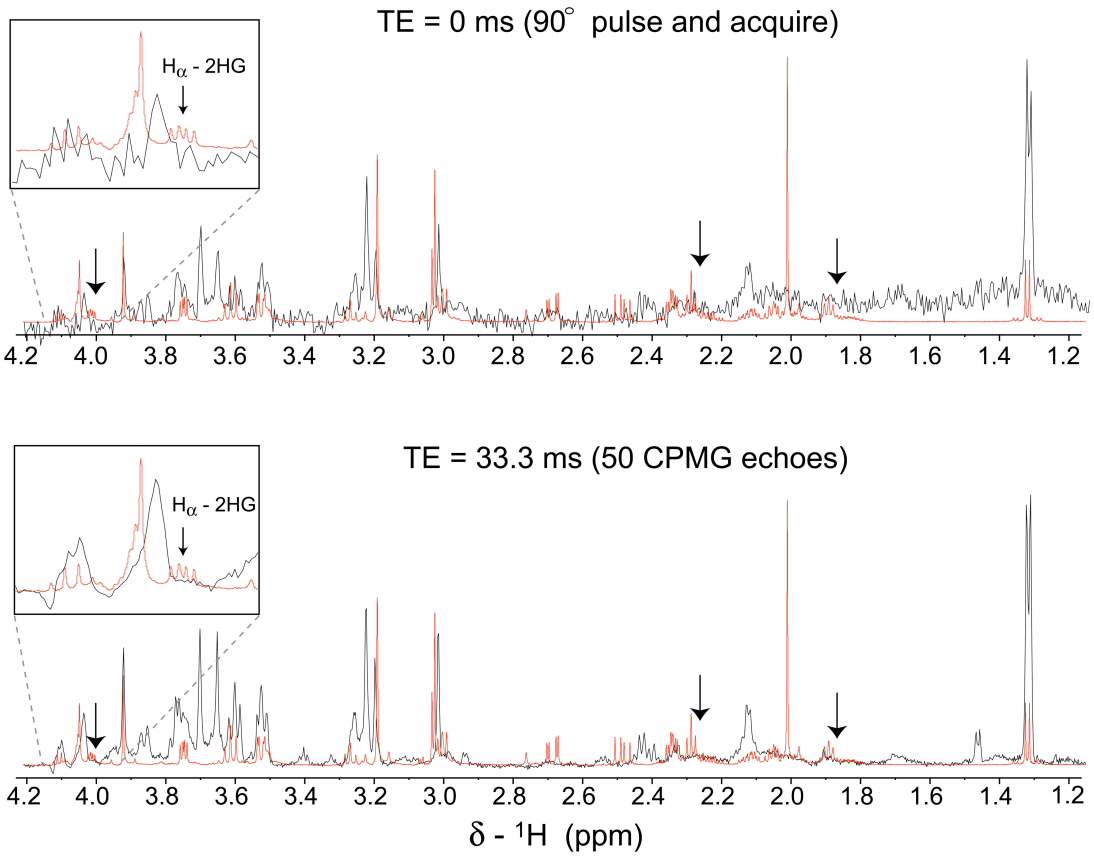

Fig. S4. 1D HRMAS spectra recorded at 14T and 3 kHz MAS on a biopsy sample from 1 patient with *IDH1*$_{R132H}$ anaplastic astrocytoma. The biopsy spectra (black trace) were overlaid with the 14T spectra of the phantom containing a mixture of normal brain metabolites and 2HG (red line). Arrows indicate the position of 2HG lines in the phantom spectrum. A zoom around the H_{α} of 2HG is shown in the insets. The 1D spectra were recorded with direct excitation experiment (pulse and acquire, echo time (TE) of 0 ms; upper spectra) and with a Carr-Purcell-Meiboom-Gill train of pulses (CPMG, 50 echoes, TE = 33.3 ms; lower spectra).

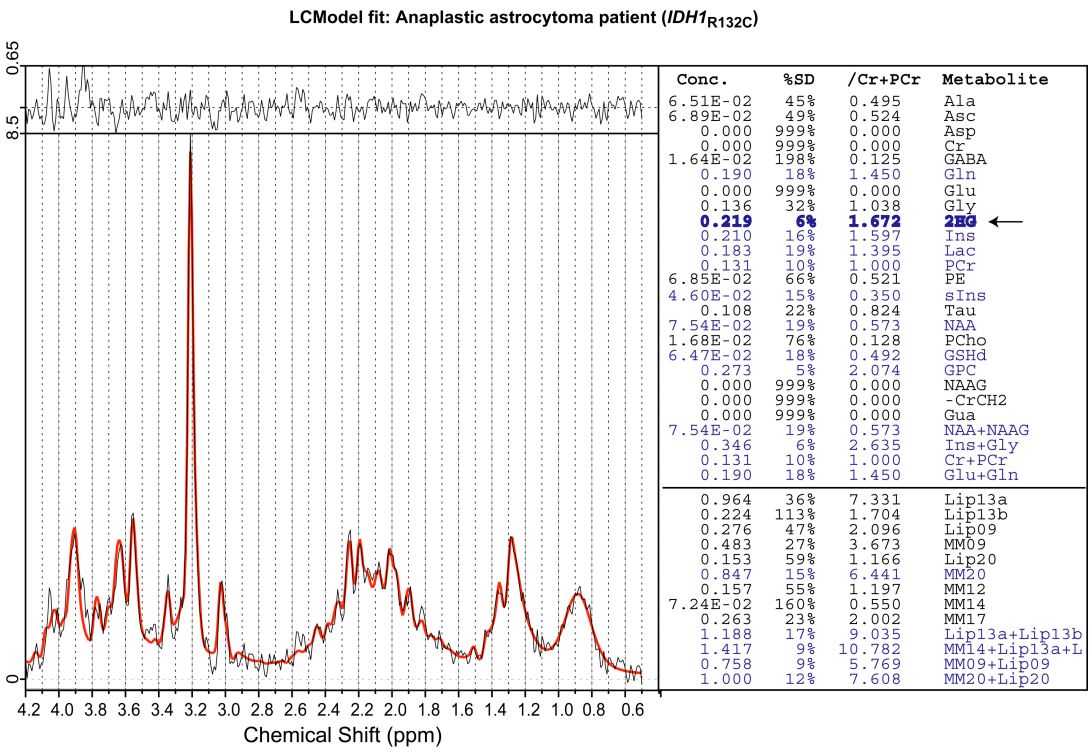

Fig. S5. LCModel fitting of the 1D LASER spectrum from the *IDH1*$_{R132C}$ anaplastic astrocytoma patient. 2HG is found by LCModel (red line computed spectrum) to be present within goodness of fit confidence limits (6% Cramer-Rao lower bounds). Arrow points to 2HG. Metabolites fitted within confidence limits (Cramer-Rao lower bounds less than 20%) are shown in blue. Experimental measured spectrum is shown as a black line, and the residual difference between measured and fitted spectra is shown above.

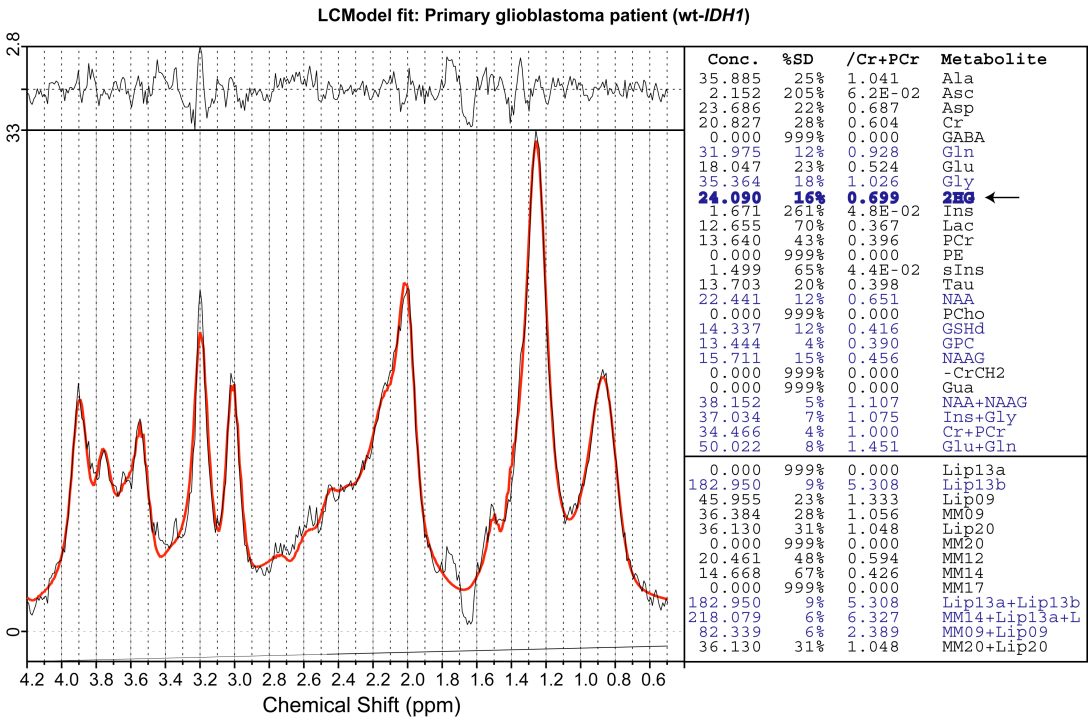

Fig. S6. LCModel fitting of the 1D LASER spectrum from a wt-*IDH1* primary gliobalstoma patient. 2HG is found by LCModel (red line computed spectrum) to be significantly present within goodness of fit confidence limits (16% Cramer-Rao lower bounds). Metabolites fitted within confidence limits (Cramer-Rao lower bounds less than 20%) are shown in blue. Experimental measured spectrum is shown in black line, and the residual difference between measured and fitted spectra is shown above.

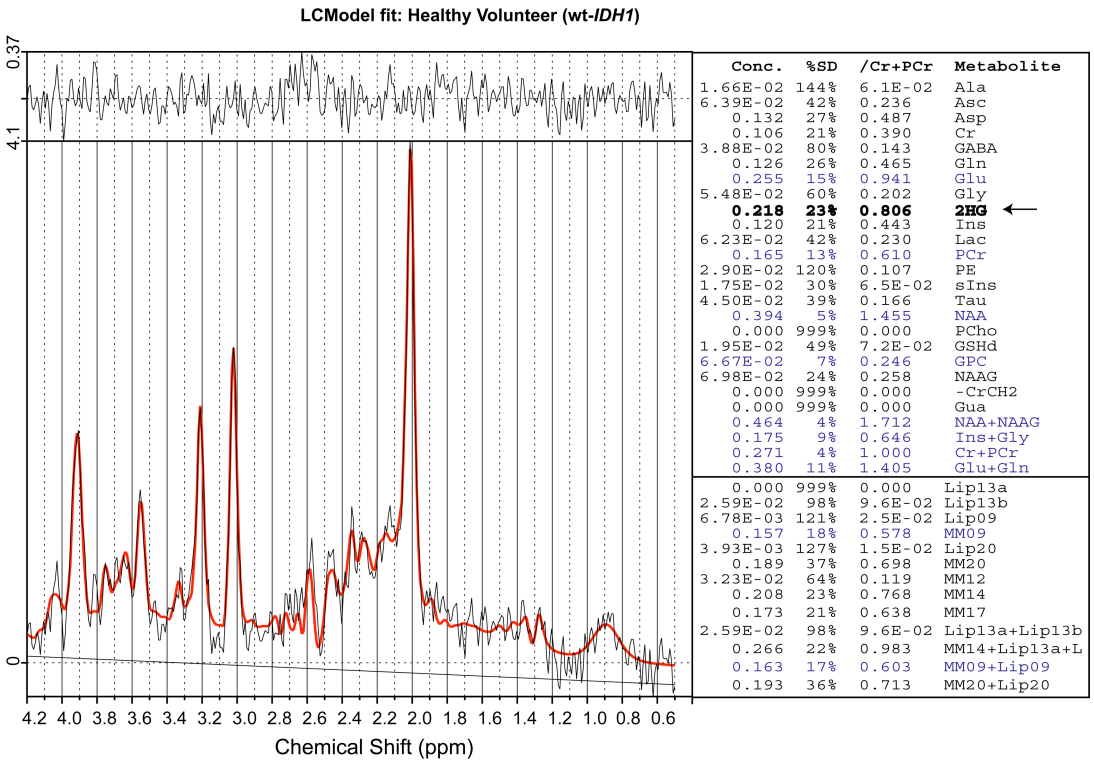

Fig. S7. LCModel fitting of the 1D LASER spectrum from a wt-*IDH1* healthy volunteer. LCModel fitting (red line computed spectrum) reports 2HG slightly outside the confidence limits for goodness of fit (23% Cramer-Rao lower bounds). Metabolites fitted within confidence limits (Cramer-Rao lower bounds less than 20%) are shown in blue. Experimental measured spectrum is shown in black line, and the residual difference between measured and fitted spectra is shown above.

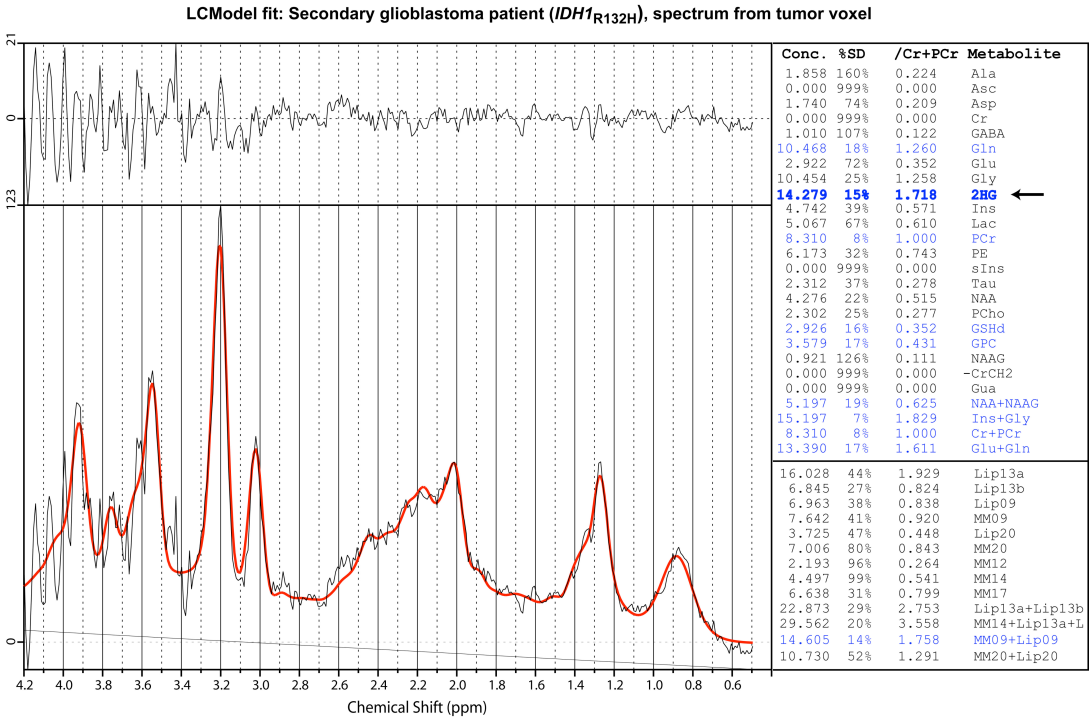

Fig. S8. LCModel fitting of the 1D LASER spectrum from the tumor voxel of the *IDH1*$_{R132H}$ secondary glioblastoma patient. 2HG is found by LCModel (red line computed spectrum) to be significantly present within goodness of fit confidence limits (15% Cramer-Rao lower bounds). Metabolites fitted within confidence limits (Cramer-Rao lower bounds less than 20%) are shown in blue. Experimental measured spectrum is shown in black line, and the residual difference between measured and fitted spectra is shown above.

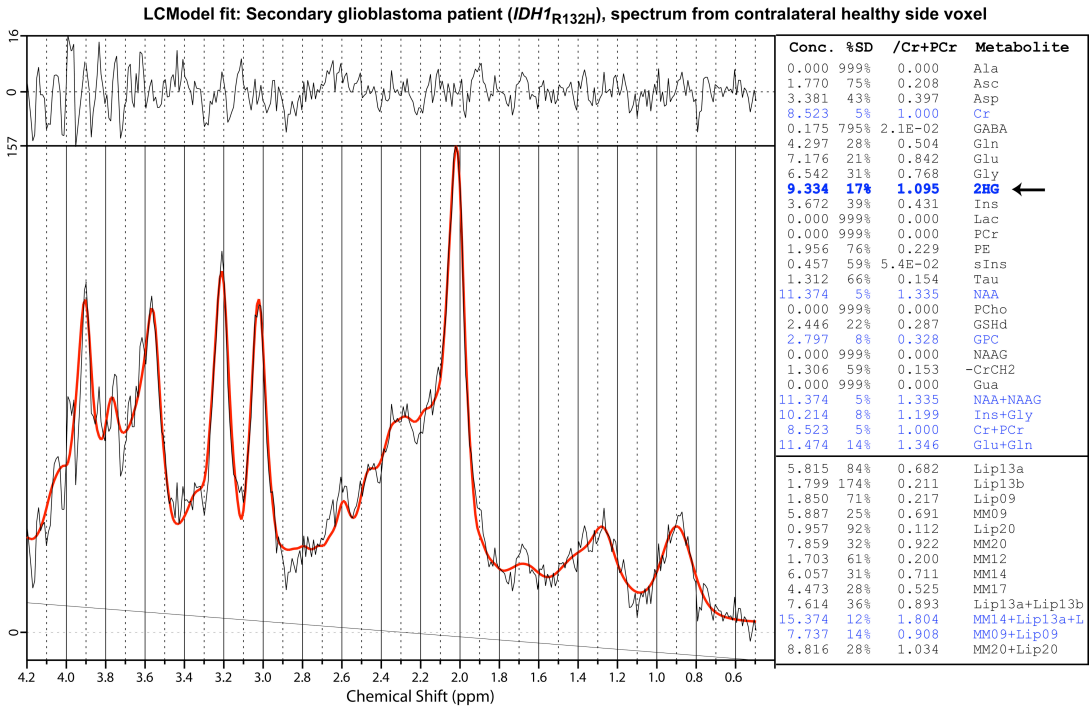

Fig. S9. LCModel fitting of the 1D LASER spectrum from the healthy side voxel of the *IDH1*$_{R132H}$ secondary glioblastoma patient. 2HG is found by LCModel (red line computed spectrum) to be significantly present within goodness of fit confidence limits (17% Cramer-Rao lower bounds). Metabolites fitted within confidence limits (Cramer-Rao lower bounds less than 20%) are shown in blue. Experimental measured spectrum is shown in black line, and the residual difference between measured and fitted spectra is shown above.

References:

1. D. Dias-Santagata, S. Akhavanfard, S. S. David, K. Vernovsky, G. Kuhlmann, S. L. Boisvert, H. Stubbs, U. McDermott, J. Settleman, E. L. Kwak, J. W. Clark, S. J. Isakoff, L. V. Sequist, J. A. Engelman, T. J. Lynch, D. A. Haber, D. N. Louis, L. W. Ellisen, D. R. Borger, A. J. Lafrate, *Embo Molecular Medicine* **2**, 146 (May, 2010).
2. O. C. Andronesi, S. Ramadan, E. M. Ratai, D. Jennings, C. E. Mountford, A. G. Sorensen, *Journal of Magnetic Resonance* **203**, 283 (Apr, 2010).
3. O. C. Andronesi, S. Ramadan, C. E. Mountford, A. G. Sorensen, *Magnetic Resonance in Medicine* **64**, 1542 (2010).
4. S. A. Smith, T. O. Levante, B. H. Meier, R. R. Ernst, *Journal of Magnetic Resonance Series A* **106**, 75 (Jan, 1994).
5. D. Bal, A. Gryff-Keller, *Magnetic Resonance in Chemistry* **40**, 533 (Aug, 2002).
6. V. Govindaraju, K. Young, A. A. Maudsley, *Nmr in Biomedicine* **13**, 129 (May, 2000).
7. S. Meiboom, D. Gill, *Review of Scientific Instruments* **29**, 688 (1958).
8. L. Braunschweiler, R. R. Ernst, *Journal of Magnetic Resonance* **53**, 521 (1983).
9. M. H. Levitt, R. Freeman, T. Frenkiel, *Journal of Magnetic Resonance* **47**, 328 (1982).
10. E. Kupce, P. Schmidt, M. Rance, G. Wagner, *Journal of Magnetic Resonance* **135**, 361 (Dec, 1998).
11. L. Dang, D. W. White, S. Gross, B. D. Bennett, M. A. Bittinger, E. M. Driggers, V. R. Fantin, H. G. Jang, S. Jin, M. C. Keenan, K. M. Marks, R. M. Prins, P. S. Ward, K. E. Yen, L. M. Liau, J. D. Rabinowitz, L. C. Cantley, C. B. Thompson, M. G. V. Heiden, S. M. Su, *Nature* **462**, 739 (Dec, 2009).
12. R. J. Ogg, P. B. Kingsley, J. S. Taylor, *Journal of Magnetic Resonance Series B* **104**, 1 (May, 1994).
13. R. Gruetter, I. Tkac, *Magnetic Resonance in Medicine* **43**, 319 (Feb, 2000).
14. A. J. W. van der Kouwe, T. Benner, D. H. Salat, B. Fischl, *Neuroimage* **40**, 559 (Apr, 2008).
15. S. W. Provencher, *Magnetic Resonance in Medicine* **30**, 672 (Dec, 1993).
16. A. Naressi, C. Couturier, J. M. Devos, M. Janssen, C. Mangeat, R. de Beer, D. Graveron-Demilly, *Magnetic Resonance Materials in Physics Biology and Medicine* **12**, 141 (May, 2001).
17. Y. Y. Lin, P. Hodgkinson, M. Ernst, A. Pines, *Journal of Magnetic Resonance* **128**, 30 (Sep, 1997).
18. M. C. Martinez-Bisbal, L. Marti-Bonmati, J. Piquer, A. Revert, P. Ferrer, J. L. Llacer, M. Piotto, O. Assemat, B. Celda, *Nmr in Biomedicine* **17**, 191 (Jun, 2004).
19. M. A. Thomas, N. Hattori, M. Umeda, T. Sawada, S. Naruse, *Nmr in Biomedicine* **16**, 245 (Aug, 2003).